



# HHS Public Access

Author manuscript

*Nat Neurosci.* Author manuscript; available in PMC 2011 January 01.

Published in final edited form as:

*Nat Neurosci.* 2010 July ; 13(7): 889–895. doi:10.1038/nn.2573.

## STIMULUS-DRIVEN COMPETITION IN A CHOLINERGIC MIDBRAIN NUCLEUS

Ali Asadollahi, Shreesh P. Mysore, and Eric I. Knudsen

Department of Neurobiology, Stanford School of Medicine, Stanford, CA 94305, USA

### Abstract

The mechanisms by which the brain selects a particular stimulus as the next target for gaze are poorly understood. A cholinergic nucleus in the owl's midbrain exhibits functional properties that suggest its role in bottom-up stimulus selection. Neurons in the nucleus isthmi pars parvocellularis (Ipc) respond to wide ranges of visual and auditory features, but they are not tuned to particular values of those features. Instead, they encode the relative strengths of stimuli across the entirety of space. Many neurons exhibit switch-like properties, abruptly increasing their responses to a stimulus in their receptive field when it becomes the strongest stimulus. This information propagates directly to the optic tectum, a structure involved in gaze control and stimulus selection, as periodic (25–50 Hz) bursts of cholinergic activity. The functional properties of Ipc neurons resemble those of a “salience map”, a core component in computational models for spatial attention and gaze control.

---

Signals from the forebrain usually dictate the next target for gaze and attention 1, 2. However, the midbrain also contains circuits that are capable of directing gaze and, under certain conditions, can select stimuli or locations as targets for gaze and attention 3–6. The central component of this midbrain circuitry is the optic tectum (superior colliculus in mammals), a multilayered structure that receives spatial information from many sensory modalities about the locations of stimuli and sends output both to the forebrain as well as to the brainstem tegmentum to control the direction of gaze 7, 8.

Bottom-up attention refers to target selection based on the relative physical salience of stimuli. In computational models, the evaluation of stimulus salience is carried out by a salience map, a topographic representation of space, consisting of “neurons” that respond to the strength of stimulus parameters, such as contrast or motion, but that are not tuned for stimulus features, such as contour orientation or motion direction 9–11. In this hypothetical salience map, neurons compare the strengths of stimuli across the entire visual field, and represent the next target for gaze and attention as the region of maximal activity in the map.

---

Users may view, print, copy, download and text and data- mine the content in such documents, for the purposes of academic research, subject always to the full Conditions of use: [http://www.nature.com/authors/editorial\\_policies/license.html#terms](http://www.nature.com/authors/editorial_policies/license.html#terms)

The authors declare no conflicts of interest.

### AUTHOR CONTRIBUTIONS

AA, SPM and EIK designed the experiments and formulated the analysis. AA performed the experiments and data analysis. EIK wrote the paper.

The optic tectum is thought to contain a salience map 12, 13. Furthermore, some have proposed that a network of cholinergic and GABAergic nuclei (collectively referred to as the isthmic nuclei), that interconnects with the optic tectum, participates in the evaluation of relative stimulus salience in the optic tectum, based on the distinctive patterns of anatomical connections among these nuclei 14–16. This attractive hypothesis has never been rigorously tested neurophysiologically.

In this study we find, in support of the hypothesis, that neurons in the cholinergic isthmic nucleus Ipc (called the parabigeminal nucleus in mammals 17) encode relative stimulus strength across sensory modalities and across the visual field. Not only do Ipc neurons exhibit all of the requisite properties of the hypothetical salience map 9, 11, they also encode an additional computational step of enhancing signaling when differences in stimulus strengths are small. This information, which results from the interactions of the various isthmic nuclei, is transmitted directly to the optic tectum by Ipc neurons containing acetylcholine, a neuromodulator that has been strongly implicated in behavioral tests of stimulus selection 18.

Bottom-up stimulus competition can be biased by top-down signals representing voluntary goals 19, and the Ipc receives direct descending projections from the owl's forebrain gaze control area that conveys top-down influences 20, 21. In order to minimize the effects of top-down signals on stimulus-driven competition, we studied competition in tranquilized owls. We found that the rules of competition were the same in both tranquilized and non-tranquilized animals. Thus, the neural correlates of stimulus competition that we report represent mechanisms that operate automatically, in a bottom-up fashion, on sensory inputs.

## RESULTS

### Ipc Responses to Single Stimuli

A previous study in the barn owl employed single visual and auditory stimuli to demonstrate that neurons in the Ipc are multimodal, respond to a variety of visual features (positive and negative contrasts; bars and spots) and auditory features (narrow-band and broad-band sounds over a range of levels), and they exhibit well-defined spatial receptive fields that are organized topographically to form a multimodal map of space 22. We confirmed and extended these observations by testing Ipc units with additional stimulus features: visual contrast, bar orientation, direction and speed of motion, and dot size. For each test, the stimulus was located at the center of the unit's visual receptive field, the region of space within which a visual stimulus drove spikes, (Methods; Supplementary Fig. 1 online).

Ipc units were sensitive to, but were not tuned for (Methods), changes in contrast (Supplementary Fig. 2a online), loom speed (Supplementary Fig. 2b online), translation speed (Supplementary Fig. 2c online), and sound level 22, with most units increasing their firing rates with increasing stimulus strength (Spearman's rank correlation,  $P < 0.05$ , contrast: 29 of 29 units; loom speed 37 of 43; translation speed: 7 out of 13); note that for both loom speed and translational speed, increasing speed also activates an increasing number of units across the space map. Ipc units were rarely selective for either motion direction (1 out of 18) or bar orientation (0 out of 14), and most responses were not even modulated by these

features (Supplementary Fig. 2e, f online; response modulation: Kruskal-Wallis test,  $P < 0.05$ , 4 out of 18 for motion direction; 3 out of 14 for bar orientation). In addition, they responded to a wide range of dot sizes, with a tendency across the population for responses to decrease to large sizes (Supplementary Fig. 2d online). The preference for small dot sizes along with the increasing responses to increasing loom speeds indicated that Ipc units responded to loom speed per se and not to the larger final dot sizes of faster looming stimuli. Thus, Ipc units are not selective for specific values of stimulus features. Rather, they increase their responses with increasing strength of intrinsically salient features, such as contrast and motion.

### Stimulus Competition Across Features and Modalities

To study stimulus competition in the Ipc, we presented the owl with paired stimuli: one stimulus ( $S_{in}$ ) was centered in the unit's receptive field and the other ( $S_{out}$  competitor; visual or auditory stimulus) was located far outside the receptive field (either  $30^\circ$  medial or lateral to the unit's receptive field center, always in the same hemifield as  $S_{in}$ ). The strength of the  $S_{in}$  stimulus was held constant while the strength of the  $S_{out}$  competitor was varied systematically, and unit responses were plotted as a competitor strength-response profile.

In the example shown (Fig. 1), the  $S_{in}$  stimulus was a dark dot that expanded (loomed) concentrically as a linear function of time. When presented alone, the looming dot evoked vigorous responses (Fig. 1, upper rasters). The features of the  $S_{out}$  competitor varied:  $S_{out}$  was either a looming dot presented at different loom speeds (Fig. 1a, lower rasters), a looming dot presented at different contrasts (Fig. 1b, lower rasters), or a broadband noise burst presented at different sound levels (Fig. 1c, lower rasters). In each case, when the  $S_{in}$  and  $S_{out}$  stimuli were presented together (Fig. 1, lower rasters), the response to the  $S_{in}$  stimulus decreased progressively as the strength of the  $S_{out}$  competitor increased (Fig. 1d; Spearman's rank correlation;  $P < 0.05$ ).

Such competitive interactions were observed across a population of 190 units tested with various combinations of stimulus features (contrast, loom speed, translational speed, and sound level; Supplementary Table 1 online). In most cases, responses to  $S_{in}$  and  $S_{out}$  presented together decreased systematically with increasing strength of the  $S_{out}$  competitor (Spearman's rank correlation,  $P < 0.05$ ; 174 out of 190 combinations of features; Supplementary Table 1 online). For the looming  $S_{out}$  competitor, the average magnitude of the suppression caused by the strongest stimulus tested ( $14^\circ/s$ ) was  $64.8\% \pm 1.7$  ( $n=135$ ). The consistently suppressive effect of various kinds of stimuli on  $S_{in}$  responses indicated that stimulus competition took place across stimulus features and across sensory modalities.

### The Ipc Signals Relative Stimulus Strength

Within the 174 feature combinations that exhibited a systematic effect of the  $S_{out}$  competitor on  $S_{in}$  responses, we observed that responses to the paired stimuli could change either gradually (Fig. 1) or abruptly (Fig. 2a–c) with increasing strength of the  $S_{out}$  competitor. To explore this phenomenon in detail, we analyzed the competitor strength-response profiles from 147 units tested with looming stimuli as both the  $S_{in}$  and  $S_{out}$  stimuli. For these measurements, the  $S_{in}$  stimulus was a looming dark dot with a loom speed that was in the

dynamic range of loom speed-response functions (Fig. 2a, Supplementary Fig. 2b online). We quantified the shape of the competitor strength-response profile by fitting average responses with a sigmoidal function (Methods), and we computed  $R^2$  as a measure of the goodness of fit to the function. Most responses were fit well by the sigmoid (median  $R^2=0.89$ ; Supplementary Fig. 3 online). We included for further analysis only responses for which  $R^2 > 0.75$  ( $n=121$ ). For these data, we derived from the sigmoidal fits the ‘transition range’: the range of competitor loom speeds that accounted for a change from 10% to 90% of the total change in suppression (Fig. 2c, dashed lines). Transition ranges were binned in increments of  $2^\circ/s$ , the resolution of our sampling.

The distribution of transition ranges was continuous, but skewed toward extremely narrow ranges (Fig. 2d). For 58% of the units (70/121), transition ranges were relatively wide, with responses decreasing gradually from strong to weak with increasing  $S_{out}$  strengths (Fig. 2d, blue). However, for the remaining 42% of the units (51/121), transition ranges were narrow, with responses changing abruptly from strong to weak with an increase in  $S_{out}$  loom speed of  $4^\circ/s$ , within two incremental steps in loom speed (Fig. 2c,d, red). Because of the abruptness of the change in responses with increasing competitor strength, we refer to these units as “switch-like units”.

Was there a relationship between the strength of the stimulus in the receptive field ( $S_{in}$ ) and the strength of the competing stimulus ( $S_{out}$ ) that caused the transition in responses from high to low? The abruptness of the response transition exhibited by switch-like units allowed us to address this question clearly. We estimated the  $S_{out}$  strength that triggered the change in the responses of switch-like units from high to low as the midpoint of the transition range (Fig. 2c, arrow), and called this  $S_{out}$  strength the ‘switch value’. We then compared the computed switch value with the strength of the  $S_{in}$  stimulus that was used to drive the unit (Fig. 2e). For most of the units (35 out of 51), the switch value was within  $2^\circ/s$  (the resolution of our measurement) of the  $S_{in}$  loom speed, and across the population, the difference between the switch value and  $S_{in}$  strength was not different from zero (Fig. 2e, red line; mean difference =  $-0.32 \pm 0.39$ ; Wilcoxon signed rank test re. zero,  $n=51$ ,  $P=0.3$ ).

These data suggest that the responses of switch-like units encoded the strength of the  $S_{out}$  stimulus relative to the strength of the stimulus located inside the unit’s receptive field. Furthermore, as a result of the switch-like transition from strong to weak responses with increasing  $S_{out}$  strength, switch-like units were particularly sensitive to changes in  $S_{out}$  strength, more so than nonswitch-like units, when the difference in the strengths of the competing stimuli was small (Fig. 2f, red versus blue curve), but less sensitive than nonswitch-like units when the competing stimulus was much stronger than the  $S_{in}$  stimulus (Fig. 2f, right side).

If switch-like units encoded the strength of the competing stimulus relative to the strength of the stimulus in their receptive fields, then an increase in the strength of the  $S_{in}$  stimulus should result in an increase in the switch value. To test this prediction, we measured competitor strength-response profiles for a subset of 13 switch-like units with two different  $S_{in}$  loom speeds (Fig. 3a). The effect of the strength of the  $S_{in}$  stimulus on the switch value was quantified as the ratio of the shift in the switch value relative to the increment in the  $S_{in}$

stimulus (Fig. 3b). On average, switch values shifted by an amount approximately equal to the  $S_{in}$  increment: mean ratio =  $0.77 \pm 0.16$  (Wilcoxon signed rank test re. 1,  $n=13$ ,  $P=0.24$ ; Wilcoxon signed rank test re. zero,  $n=13$ ,  $P<0.002$ ; Fig. 3b, solid line). Thus, switch-like units did indeed signal the strength of the competing stimulus relative to the strength of the stimulus in their receptive fields, and they also exhibited enhanced discriminability of the strength of a competing stimulus when the difference in the strengths of stimuli is small (Fig. 2f, red circles).

Although this property of switch-like units is reminiscent of hypothetical, winner-take-all neurons in computational networks that select the strongest stimulus for gaze or spatial attention 9, 11, switch-like units did not act in a winner-take-all fashion. Responses to the paired  $S_{in}$  and  $S_{out}$  stimuli were consistently greater with a strong  $S_{in}$  stimulus (Fig. 3a, filled circles) than with a weak  $S_{in}$  stimulus (Fig. 3b, open circles). Consequently, unlike with putative winner-take-all units, switch-like units continued to encode the absolute strength of the  $S_{in}$  stimulus, even when it was the “loser” stimulus (Fig. 3a; compare rightmost points, filled vs. open circles; Fig. 3c, black bars). The same was true of nonswitch-like units (Fig. 3c, gray bars). Thus, both switch-like and nonswitch-like units encoded both the absolute strength of a receptive field stimulus as well as its strength relative to that of a competing stimulus.

### Global Stimulus Competition

Finally, we tested the spatial extent of stimulus competition by measuring the effect of an  $S_{out}$  stimulus, presented at various locations outside the receptive field, on the responses to a standard  $S_{in}$  stimulus for 31 Ipc units. The standard  $S_{in}$  stimulus was a looming dark dot with a loom speed that evoked 50% of the maximum loom response; the competing  $S_{out}$  stimulus was a dark dot that loomed at a speed that was 4 °/s faster than the speed of the  $S_{in}$  stimulus. When either stimulus was located inside the receptive field, each drove the unit well (Fig. 4a,b). However, the vigorous responses to the  $S_{in}$  stimulus alone (Fig. 4a, upper raster) were suppressed (Kruskal-Wallis, multiple comparisons,  $P<0.05$ ), when the  $S_{out}$  stimulus was located anywhere lateral to the receptive field or medial to the receptive field and  $<15^\circ$  into the opposite hemifield (Fig. 4c, red circles); these locations are represented in the space map on the same side of the brain 23. For this unit, response suppression was not significantly different from zero for individual locations  $15^\circ$  into the opposite hemifield (Fig. 4c, blue circles), but was significantly different from zero when the responses to these locations were combined (Wilcoxon signed rank test,  $P<0.05$ ).

The suppression of responses to the  $S_{in}$  stimulus by a competing  $S_{out}$  stimulus varied in efficacy across different units and, for each unit, across different  $S_{out}$  locations. Population analysis revealed, however, that average suppression did not differ systematically (Kruskal-Wallis,  $n=31$ ,  $P=0.12$ ) for competitor  $S_{out}$  stimuli located more than  $15^\circ$  in azimuth or elevation from the center of the receptive field, as long as the  $S_{out}$  stimulus was located in the same hemifield as the  $S_{in}$  stimulus or  $<15^\circ$  into the opposite hemifield (Fig. 4d, red circles):  $S_{out}$  locations medial or lateral to the receptive field suppressed responses by  $75.9\% \pm 2.4$  (Wilcoxon rank sum test,  $n=31$ ,  $P<0.0001$ ), and  $S_{out}$  locations above or below the receptive field suppressed responses by  $69.2\% \pm 3.2$  (Fig. 4e; Wilcoxon rank sum test,  $n=24$ ,

$P < 0.0001$ ). In contrast, the suppressive effect of an  $S_{out}$  stimulus decreased dramatically when it was located  $15^\circ$  into the opposite hemifield (Fig. 4d, blue circles). For these locations, the  $S_{out}$  competitor suppressed responses to  $S_{in}$  by an average of only  $27.6\% \pm 3.7$  (Wilcoxon rank sum test,  $n=31$ ,  $P < 0.0001$ ). Because these locations are not represented in the space map on the same side of the brain 22, 23, we refer to them as being on the “opposite side” relative to the  $S_{in}$  stimulus. Conversely, when  $S_{out}$  stimuli were located  $<15^\circ$  into the opposite hemifield, we refer to them as being on the “same side” as the  $S_{in}$  stimulus.

We further explored the decreased inhibitory effect of a competing stimulus when  $S_{out}$  was located on the opposite side from the  $S_{in}$  stimulus in a subset of units ( $n=17$ ) that had receptive fields located near the midline (azimuth  $< 15^\circ$ ). We measured competitor strength-response profiles with  $S_{out}$  located  $30^\circ$  on either side of the receptive field (“same side” and “opposite side” relative to the receptive field) on interleaved trials. When  $S_{in}$  and  $S_{out}$  were located on the same side, all units were powerfully inhibited by a strong  $S_{out}$  stimulus (average maximum suppression =  $71 \pm 3.7\%$ ; Supplementary Fig. 4 online, red circles), and the competitor strength-response profiles for 7 of the units (41%) were switch-like. In contrast, when  $S_{in}$  and  $S_{out}$  were located on opposite sides, maximum suppression averaged only  $4.5\% \pm 4.7$  (Wilcoxon signed rank test re. zero,  $P=0.35$ ; Wilcoxon signed rank test compared to responses with  $S_{out}$  on the same side,  $n=17$ ,  $P < 0.0001$ ; Supplementary Fig. 4 online, blue circles), and only one of these units exhibited a systematic effect of  $S_{out}$  on responses to  $S_{in}$ . Although suppression by  $S_{out}$  located on the opposite side was far weaker than suppression by  $S_{out}$  on the same side, the strengths of the suppressive effects by  $S_{out}$  on either side were correlated (correlation analysis, *corrcoef* command in MATLAB,  $r=0.63$ ,  $P < 0.001$ ).

The average maximum suppression measured when  $S_{out}$  was located on the opposite side was substantially less when assessed with competitor strength-response profiles (4.5%; Supplementary Fig. 4b online, blue circles) than it was when assessed from surveys of global stimulus competition (27.6%; Fig. 4d, blue circles; t-test,  $P < 0.01$ ). In contrast, the average maximum suppression when  $S_{out}$  was located on the same side was not different when assessed using the two different protocols (71%, Supplementary Fig. 4b online, red circles versus 75.9%, Fig. 4d, red circles;  $P > 0.05$ ). The difference between these measurement protocols was that the former involved repeated presentations of the  $S_{out}$  stimulus from the same region of space, whereas the later involved roving the  $S_{out}$  stimulus across the visual field. These data indicate, therefore, that inhibition that originated from activity on the opposite side of the brain adapted to repeated presentations of  $S_{out}$  from the same region space far more than did inhibition that originated from activity on the same side of the brain.

In summary, Ipc responses were modulated by the presence of a second stimulus located anywhere in the visual field (Fig. 4). However, the suppressive effect of a competing stimulus was far more powerful, less subject to adaptation, and could be switch-like, only when the competing stimulus was represented in the map on the same side of the brain.

## Effects of Tranquilization

Competitive interactions in the Ipc measured in owls ( $n=3$ ) that were not tranquilized were similar to those measured in tranquilized owls. For these experiments, the owls were anesthetized only during set-up (Methods), and nitrous oxide as well as anesthesia was discontinued during data collection. For these measurements, the competing  $S_{out}$  stimulus was always located on the same side as the  $S_{in}$  stimulus.

In the non-tranquilized owls, responses to a looming  $S_{in}$  stimulus were inhibited by a strong  $S_{out}$  stimulus for 36 out of 38 units (correlation analysis;  $P<0.05$ ). Among those that were inhibited, maximum suppression averaged  $63.3 \pm 3.2\%$  (s.e.m., range = 35 to 100%). The distribution of transition ranges extended from  $<2^\circ/s$  to  $12^\circ/s$ , but was skewed toward narrow ranges (Fig. 2 d, light colored bars). The inhibition of 13 units (40%) was switch-like. Among the switch-like units, switch values for 8 units were within  $2^\circ/s$  of the  $S_{in}$  loom speed, and across all of the switch-like units, switch values were not different from the strength of  $S_{in}$  (mean difference =  $-1.12 \pm 0.64$ , Wilcoxon signed rank test re. zero,  $n=13$ ,  $P=0.19$ ; Fig. 2 e, light red).

## Ipc Units Responded with Periodic Bursts of Spikes

A conspicuous property of Ipc units is that they tend to fire in high frequency (300–800 Hz) bursts of action potentials 22, 24. When driven by a stimulus inside their receptive fields, Ipc units discharged bursts of spikes periodically with a periodicity that ranged from 25 to 50 Hz (Fig. 5a–c). The power in this periodicity covaried with unit spike rates (Fig. 5d). Consequently, for switch-like units, just as response rates declined abruptly with increasing strengths of a competing  $S_{out}$  stimulus, so too did the power in this periodicity. Thus, Ipc units transmit information about the relative strengths of competing stimuli as periodic (25–50 Hz) bursts of cholinergic input to the optic tectum.

## DISCUSSION

The results from this study, combined with those reported previously 22, demonstrate that the Ipc is a topographically organized space map that represents the comparison of stimulus strengths across a range of visual and auditory features, and across all of space. Ipc units respond to, but are not selective for, a range of stimulus features, and they respond with increasing firing rates to increasing stimulus contrast and motion, two features that are intrinsically salient to animals. The responses of Ipc units to stimuli in their receptive fields are altered systematically, and sometimes dramatically, depending on the relative strength of competing stimuli. These properties reflect the interactions of the Ipc with the other isthmic nuclei and with the optic tectum itself.

According to computational models of bottom-up stimulus selection, a salience map is a topographic representation of space, in which neurons respond to the salience of stimuli, but are not tuned to particular values of stimulus features 9–11. The similarity of the properties of this hypothetical salience map with those of Ipc units is striking. The Ipc sends information directly to the optic tectum, a structure that also exhibits a salience map 12, 13 and that has been shown to contribute to stimulus selection both for gaze and attention in

behaving monkeys 3, 4. Similar salience maps have been proposed for thalamic and forebrain structures as well 12, 25. Interestingly, all of these structures connect, directly or indirectly, with the optic tectum 26, 27. In the lateral intraparietal area in monkeys, where the representation of salience has been the most thoroughly studied, stimulus salience is encoded by the relative (and not absolute) amounts of activity across the representation of space 28, as in the Ipc. Thus, the Ipc is one node in a network of structures that appears to encode the relative salience of stimuli in the world.

The degree to which stimuli interact competitively in the Ipc depends on the positions of the stimuli relative to the owl. When stimuli are both located in the same hemifield, competitive inhibition can be extremely strong, switch-like, and relatively resistant to adaptation. Inhibition is substantially weaker when stimuli are located in opposite hemifields and  $15^\circ$  from the midline. Thus, stimuli located in the same hemifield compete far more stringently for representation in the isthmotectal circuit than do stimuli that are located in opposite hemifields.

In computational models, a winner-take-all process selects the next target for gaze and spatial attention based on activity levels in a salience map. The original hypothesis<sup>14</sup> that the isthmotectal circuit might act as a hypothetical, winner-take-all network for guiding gaze and spatial attention was based on patterns of anatomical interconnections (Supplementary Fig. 5 online). The cholinergic Ipc, the GABAergic nucleus isthmi pars magnocellularis (Imc), and the optic tectum each contains a topographic map of the visual field 7, 22, 29. The Ipc map connects in a precisely reciprocal, point-to-point fashion with the optic tectum 15. The Imc also receives topographic input from the optic tectum, but Imc neurons send their axons to all portions of the space maps in both the optic tectum and Ipc, except the portion that provided their input. Many authors have pointed out that if the point-to-point connections between the optic tectum and the Ipc are excitatory, they could focally augment responses through positive feedback, while the broadly projecting GABAergic neurons from the Imc could suppress all but the most active optic tectum and Ipc neurons 14–17. Although some neurophysiological evidence is consistent with winner-take-all competition in the isthmotectal circuit 16, such a rule cannot be demonstrated without measuring the effects of parametric variations in the relative strengths of competing stimuli.

The properties of switch-like units are computationally closer to a winner-take-all process than are those of nonswitch-like units. However, the responses of switch-like Ipc units are not winner-take-all, because they continue to encode information about the absolute strength of a stimulus when the stimulus is either the “winner” or the “loser”. Instead, switch-like units provide enhanced signaling of the stronger stimulus, especially when differences in stimulus strength are small, and may set the stage for the winner-take-all computation that must precede the encoding of a change in the locus of spatial attention or gaze.

The functional properties of Ipc units are extraordinary in several respects. Global inhibition in the Ipc operates across the entire map of space (Fig. 4), enables a single discrete stimulus to powerfully suppress responses to other stimuli, and operates across stimulus features and sensory modalities (Fig. 1). Similar inhibition has been reported in the optic tectum 13, 30. In addition, global inhibition in the Ipc can cause the abrupt suppression of responses of

switch-like units by a small increment in the strength of a single competing stimulus (Fig. 2), a property distinct from typical effects of divisive normalization of neural activity 31, 32.

Another unusual property of Ipc neurons is that they are cholinergic 22, 33. Because they provide cholinergic input to the optic tectum, their activity has the potential of simultaneously increasing the sensitivity of neurons to sensory input, through pre-synaptic facilitation of excitatory circuits 34, and sharpening the spatial tuning of neurons through activation of local lateral inhibitory circuits 35. Increases in neuronal sensitivity and sharpening of spatial tuning are two consequences of stimulus selection in behaving monkeys 2 and of microstimulation-induced, top-down modulation of sensory responses in the optic tectum 36.

Finally, Ipc units respond to stimuli with conspicuously periodic (25–50 Hz) bursts of spikes (Fig. 5). Stimulus-driven activity from the Ipc to the optic tectum, that is periodic in this frequency band, has been shown to be exceptionally effective in gating ascending visual information to the thalamus, on the way to the forebrain 16. Oscillatory LFPs in this frequency band (low gamma-band) has been linked to stimulus selection in a range of structures and species 37–39.

The coexistence of these unusual properties, all of which have been associated with stimulus selection or spatial attention in a variety of independent experimental paradigms, supports the hypothesis that the Ipc plays a critical role in the bottom-up control of gaze and attention. Behavioral studies are necessary to test this hypothesis.

## METHODS

### Surgical Preparation

Twelve adult barn owls were used in this study. Bird care and surgical and experimental procedures were approved by the Stanford University Institutional Animal Care and Use Committee and were in accordance with the National Institutes of Health and the Society for Neuroscience guidelines for the care and use of laboratory animals.

Owls were prepared for multiple electrophysiological experiments. Before the first experiment, an owl was anesthetized with isoflurane (1.5%) and a mixture of nitrous oxide and oxygen (45:55), and a headbolt was mounted at the rear of the skull. Plastic cylinders were implanted over the tectal lobes. Polysporin antibiotic ointment was applied to the exposed brain surface, and the recording chambers were sealed. All wounds were cleansed with betadine and infused with a local analgesic. After recovering from surgery, the owl was returned to its flight room.

On the day of an experiment, the owl was anesthetized with isoflurane and a mixture of nitrous oxide and oxygen (45:55) and was placed in a restraining tube in prone position inside a sound-attenuating booth. The head was secured to a stereotaxic device, and the visual axes were aligned relative to a calibrated tangent screen (the eyes of the owl are essentially stationary in the head). Isoflurane was discontinued and owls were maintained in a sedated condition with the mixture of nitrous oxide and oxygen through the end of the

experiment. In five experiments, we tested unit responses in non-tranquilized owls. Three unusually calm owls were selected for these experiments. In these experiments, nitrous oxide was also discontinued during the measurements.

## Neurophysiology

Epoxy-coated tungsten microelectrodes, with high impedance (10–15 M $\Omega$  at 1kHz, FHC, Bowdoinham, ME), were used to record extracellularly from single Ipc units. Units were isolated based on spike waveform. Spikes were recorded from 400 ms before stimulus onset until 600 ms after stimulus onset. Spike times were stored using Tucker-Davis hardware (RA-16, Tucker Davis Technologies, Alachua, FL) controlled by customized MATLAB (The Mathworks, Inc., Natick, MA) software.

## Visual and auditory stimulation

Visual and auditory stimuli were presented for 250 ms. Inter-stimulus intervals ranged from 2.5 to 5.0 s, and the number of trials repeated for a given condition ranged from 10–25.

Visual stimuli were created using customized MATLAB software (courtesy of Joe Bergan) and psychophysics toolbox extensions and presented (Mitsubishi XD300U projector) on a calibrated tangent screen 35 cm from the eyes. The owl was positioned so that the visual axes were in the horizontal plane aligned with 0° elevation and 0° azimuth of the screen. All locations are given in double pole coordinates of azimuth, relative to the midsagittal plane, and elevation, relative to the visual plane. Stationary dots: black dot (1.5° radius) on a gray background. Stationary bars: black rectangular bar, 4° length and 1° width on a gray background. Looming dots: black dot on a gray background. The size of the dot increased linearly over the period of stimulus presentation (250 ms) starting from a size of 0.6° radius. Loom speeds ranged from 0 deg/s to 14 deg/s. Different loom speeds were achieved by changing the final size of the dot (from 0.6° to 4.1°), while keeping the initial size (0.6°) and the duration of presentation (250 ms) fixed.

Auditory stimuli were presented in virtual space through earphones. Waveforms simulating flat spectrum ( $\pm 2$  dB; 2–10 kHz) noise bursts (5 ms rise/fall time) were generated using customized MATLAB software interfaced with Tucker Davis Technologies hardware (RP2). The waveforms were filtered with head-related transfer functions from a typical barn owl 40 and delivered binaurally through matched earphones (ED-1914; Knowles Electronics, Itasca, IL) coupled to damping assemblies (BF-1743) inserted into the ear canals ~5mm from the eardrums. Sound levels were equalized to within  $\pm 2$  dB across the earphones, and are reported in dB relative to threshold for each unit.

To assess the receptive field of a unit, first we estimated the location of the receptive field by manually moving a visual or auditory stimulus across the visual field. Then we presented a 6°/s looming dot stimulus randomly at different azimuths (elevations) at a fixed elevation (azimuth). The center of the receptive field was calculated as the weighted average of these responses. To measure the response function of a unit to a single visual stimulus with different feature values, we presented the stimulus near the center of the receptive field.

To measure the spatial profile of competition, we presented one looming stimulus inside the receptive field ( $S_{in}$ ) and a second looming stimulus at different locations outside the receptive field ( $S_{out}$ ). The loom speeds of the two stimuli were constant, and the  $S_{out}$  was always stronger than the  $S_{in}$  stimulus.

To measure the effects of  $S_{out}$  strength on responses to an  $S_{in}$  stimulus (competitor strength-response profiles),  $S_{in}$  was a standard looming stimulus presented inside the receptive field while  $S_{out}$  stimuli of various strengths were presented at a fixed location far outside the receptive field,  $30^\circ$  from the receptive field center. This protocol yielded a competitor strength-response profile. For units with laterally located receptive fields (center  $> 20^\circ$  azimuth),  $S_{out}$  was always positioned medial to the receptive field. For units with frontally located receptive fields (center  $< 20^\circ$  azimuth),  $S_{out}$  was always positioned further lateral, and for a subset of these units ( $n = 17$ ),  $S_{out}$  was positioned both further lateral and in the opposite hemifield on interleaved trials. In some cases the  $S_{out}$  was a moving dot with variable speed, a looming dot with variable contrast and fixed loom speed, or a noise burst with variable intensity. Responses to  $S_{in}$  alone served as control and were recorded in an interleaved way with the two-stimulus configuration.

To minimize habituation to the  $S_{in}$  and  $S_{out}$  stimuli, the locations of the stimuli were jittered on subsequent presentations within a small region around the given value whenever locations were sampled repeatedly.

## Data analysis

All data analysis and presentation were performed using MATLAB. Net responses were quantified by subtracting the average firing rate during the pre-stimulus period across all interleaved trials (baseline activity) from the average firing rate during a fixed window after stimulus onset. For response functions to a single stimulus, a post-stimulus spike count window of 0–250 ms was used. For two-stimulus experiments involving paired visual stimuli, a spike count window of 100–250 ms was used, both for the paired stimuli and for the interleaved, single  $S_{in}$  stimulus. When an auditory stimulus was paired with a visual stimulus, responses were counted 40–200 ms after stimulus onset.

We used a Lilliefors test (*lillietest* command in MATLAB) to evaluate the normality of sample distributions. When a distribution was normal (Lilliefors test,  $P < 0.05$ ) and the sample size was large ( $n > 15$ ), we used parametric tests (ANOVA or t-test, *anova1* or *ttest* commands in MATLAB) to test for significance, otherwise we used non-parametric tests (Kruskal-Wallis or Wilcoxon tests, *kruskalwallis* or *ranksum* or *signrank* commands in MATLAB). Whenever we report data as  $a \pm b$ ,  $a$  is the mean and  $b$  is the standard error of mean (s.e.m.).

Responses were considered to be sensitive to a stimulus feature if the responses were significantly correlated (Spearman's rank correlation test,  $P < 0.05$ , *corr* command in MATLAB, test type Spearman) to feature values. Responses were considered to be tuned to a stimulus feature if the peak response was flanked on both sides by responses less than the half-peak value. Responses that did not yield a significant effect of feature value based on the Kruskal-Wallis test were considered to be not modulated by the feature. Responses to

loom speed, contrast, dot size, and translation speed typically yielded a significant correlation (sensitive), but were not tuned since they exhibited peaks that were flanked only on one side by responses less than the half-peak value. Responses to bar orientation and motion direction were typically not modulated: no significant effect based on Kruskal-Wallis test.

Responses that exhibited a significant correlation with competitor strength were fit (using *nlinfit* command in MATLAB) with the following sigmoidal function:

$$r(x) = c + \frac{s}{(1 + e^{-m(x-d)})}$$

where  $r(x)$  = average response to loom speed  $x$ ,  $c$ =minimum response;  $s$ =maximum response;  $d$ =speed for maximum slope (switch value);  $m$ =slope parameter.

We calculated the discrimination index ( $d'$ ) between the responses to every increment in  $S_{out}$  value from competitor strength-response profiles, using the following formula:

$$d' = \frac{\mu_2 - \mu_1}{\sqrt{\sigma_1^2 + \sigma_2^2}}$$

$\mu_1$  and  $\mu_2$  are the mean responses to data sets 1 and 2, respectively, and  $\sigma_1$  and  $\sigma_2$  are the standard deviations of those data sets.

For spectral analysis of periodic bursting, responses were evaluated during a post-stimulus period of 100–250 ms. Spike spectrum was estimated with the multitaper method (Chronux, <http://chronux.org>), using 5 tapers, resulting in a spectral resolution of 10 Hz. 95% confidence intervals were estimated using the jackknife procedure.

## Supplementary Material

Refer to Web version on PubMed Central for supplementary material.

## ACKNOWLEDGMENTS

We thank P. Knudsen for technical support, C. Goddard and S. Devarajan for helpful discussions and T. Moore, B. Noudoost and N. Steinmetz for reviewing the manuscript. The research was supported by grants from the National Institutes of Health (R01 EY019179) to EIK.

## REFERENCES

1. Sommer MA, Wurtz RH. Composition and topographic organization of signals sent from the frontal eye field to the superior colliculus. *J Neurophysiol.* 2000; 83:1979–2001. [PubMed: 10758109]
2. Reynolds JH, Chelazzi L. Attentional modulation of visual processing. *Annu Rev Neurosci.* 2004; 27:611–647. [PubMed: 15217345]
3. McPeck RM, Keller EL. Saccade target selection in the superior colliculus during a visual search task. *J Neurophysiol.* 2002; 88:2019–2034. [PubMed: 12364525]

4. Muller JR, Philiastides MG, Newsome WT. Microstimulation of the superior colliculus focuses attention without moving the eyes. *Proc Natl Acad Sci U S A*. 2005; 102:524–529. [PubMed: 15601760]
5. Schiller PH, Sandell JH, Maunsell JH. The effect of frontal eye field and superior colliculus lesions on saccadic latencies in the rhesus monkey. *J Neurophysiol*. 1987; 57:1033–1049. [PubMed: 3585453]
6. Knudsen EI, Knudsen PF. Contribution of the forebrain archistriatal gaze fields to auditory orienting behavior in the barn owl. *Exp. Brain Res*. 1996; 108:23–32. [PubMed: 8721152]
7. Stein, BE.; Meredith, MA. *The Merging of the Senses*. Cambridge, MA: MIT Press; 1993.
8. Sparks DL. The brainstem control of saccadic eye movements. *Nat Rev Neurosci*. 2002; 3:952–964. [PubMed: 12461552]
9. Itti L, Koch C. Computational modelling of visual attention. *Nat Rev Neurosci*. 2001; 2:194–203. [PubMed: 11256080]
10. Itti L, Koch C. A saliency-based search mechanism for overt and covert shifts of visual attention. *Vision Res*. 2000; 40:1489–1506. [PubMed: 10788654]
11. Parkhurst D, Law K, Niebur E. Modeling the role of salience in the allocation of overt visual attention. *Vision Res*. 2002; 42:107–123. [PubMed: 11804636]
12. Fecteau JH, Munoz DP. Saliency, relevance, and firing: a priority map for target selection. *Trends Cogn Sci*. 2006; 10:382–390. [PubMed: 16843702]
13. Mysore SP, Asadollahi A, Knudsen EI. Global inhibition and stimulus competition in the owl optic tectum. *J Neurosci*. 2010; 30:1727–1738. [PubMed: 20130182]
14. Sereno MI, Ulinski PS. Caudal topographic nucleus isthmi and the rostral nontopographic nucleus isthmi in the turtle, *Pseudemys scripta*. *J Comp Neurol*. 1987; 261:319–346. [PubMed: 3611415]
15. Wang Y, Luksch H, Brecha NC, Karten HJ. Columnar projections from the cholinergic nucleus isthmi to the optic tectum in chicks (*Gallus gallus*): a possible substrate for synchronizing tectal channels. *J Comp Neurol*. 2006; 494:7–35. [PubMed: 16304683]
16. Marin G, et al. A cholinergic gating mechanism controlled by competitive interactions in the optic tectum of the pigeon. *J Neurosci*. 2007; 27:8112–8121. [PubMed: 17652602]
17. Wang SR. The nucleus isthmi and dual modulation of the receptive field of tectal neurons in non-mammals. *Brain Res Brain Res Rev*. 2003; 41:13–25. [PubMed: 12505645]
18. Sarter M, Hasselmo ME, Bruno JP, Givens B. Unraveling the attentional functions of cortical cholinergic inputs: interactions between signal-driven and cognitive modulation of signal detection. *Brain Res Brain Res Rev*. 2005; 48:98–111. [PubMed: 15708630]
19. Goldberg ME, Wurtz RH. Activity of superior colliculus in behaving monkey. II. Effect of attention on neuronal responses. *J Neurophysiol*. 1972; 35:560–574. [PubMed: 4624740]
20. Knudsen EI, Cohen YE, Masino T. Characterization of a forebrain gaze field in the archistriatum of the barn owl: microstimulation and anatomical connections. *J Neurosci*. 1995; 15:5139–5151. [PubMed: 7623141]
21. Winkowski DE, Knudsen EI. Top-down control of multimodal sensitivity in the barn owl optic tectum. *J Neurosci*. 2007; 27:13279–13291. [PubMed: 18045922]
22. Maczko KA, Knudsen PF, Knudsen EI. Auditory and visual space maps in the cholinergic nucleus isthmi pars parvocellularis of the barn owl. *J Neurosci*. 2006; 26:12799–12806. [PubMed: 17151283]
23. Knudsen EI. Auditory and visual maps of space in the optic tectum of the owl. *J. Neurosci*. 1982; 2:1177–1194. [PubMed: 7119872]
24. Marin G, Mpodozis J, Sentis E, Ossandon T, Letelier JC. Oscillatory bursts in the optic tectum of birds represent re-entrant signals from the nucleus isthmi pars parvocellularis. *J Neurosci*. 2005; 25:7081–7089. [PubMed: 16049185]
25. Goldberg ME, Bisley J, Powell KD, Gottlieb J, Kusunoki M. The role of the lateral intraparietal area of the monkey in the generation of saccades and visuospatial attention. *Ann N Y Acad Sci*. 2002; 956:205–215. [PubMed: 11960805]
26. Shipp S. The brain circuitry of attention. *Trends Cogn Sci*. 2004; 8:223–230. [PubMed: 15120681]

27. Karten HJ. Organization of avian telencephalon and some speculations on phylogeny of amniote telencephalon. *Ann N Y Acad Sci.* 1969; 167:164–179.
28. Bisley JW, Goldberg ME. Neuronal activity in the lateral intraparietal area and spatial attention. *Science.* 2003; 299:81–86. [PubMed: 12511644]
29. Yan K, Wang SR. Visual responses of neurons in the avian nucleus isthmi. *Neurosci Lett.* 1986; 64:340–344. [PubMed: 2421216]
30. Rizzolatti G, Camarda R, Grupp LA, Pisa M. Inhibitory effect of remote visual stimuli on visual responses of cat superior colliculus: spatial and temporal factors. *J Neurophysiol.* 1974; 37:1262–1275. [PubMed: 4436699]
31. Carandini M, Heeger DJ. Summation and division by neurons in primate visual cortex. *Science.* 1994; 264:1333–1336. [PubMed: 8191289]
32. Marino J, et al. Invariant computations in local cortical networks with balanced excitation and inhibition. *Nat Neurosci.* 2005; 8:194–201. [PubMed: 15665876]
33. Sorenson EM, Parkinson D, Dahl JL, Chiappinelli VA. Immunohistochemical localization of choline acetyltransferase in the chicken mesencephalon. *J Comp Neurol.* 1989; 281:641–657. [PubMed: 2708587]
34. Yu CJ, Debski EA. The effects of nicotinic and muscarinic receptor activation on patch-clamped cells in the optic tectum of rana pipiens. *Neuroscience.* 2003; 118:135–144. [PubMed: 12676145]
35. Endo T, Yanagawa Y, Obata K, Isa T. Nicotinic acetylcholine receptor subtypes involved in facilitation of GABAergic inhibition in mouse superficial superior colliculus. *J Neurophysiol.* 2005; 94:3893–3902. [PubMed: 16107532]
36. Winkowski DE, Knudsen EI. Distinct mechanisms for top-down control of neural gain and sensitivity in the owl optic tectum. *Neuron.* 2008; 60:698–708. [PubMed: 19038225]
37. Buschman TJ, Miller EK. Top-down versus bottom-up control of attention in the prefrontal and posterior parietal cortices. *Science.* 2007; 315:1860–1862. [PubMed: 17395832]
38. Fries P, Reynolds JH, Rorie AE, Desimone R. Modulation of oscillatory neuronal synchronization by selective visual attention. *Science.* 2001; 291:1560–1563. [PubMed: 11222864]
39. Lakatos P, Karmos G, Mehta AD, Ulbert I, Schroeder CE. Entrainment of neuronal oscillations as a mechanism of attentional selection. *Science.* 2008; 320:110–113. [PubMed: 18388295]
40. Witten IB, Knudsen PF, Knudsen EI. A dominance hierarchy of auditory spatial cues in barn owls. *PLoS One.* (in press).

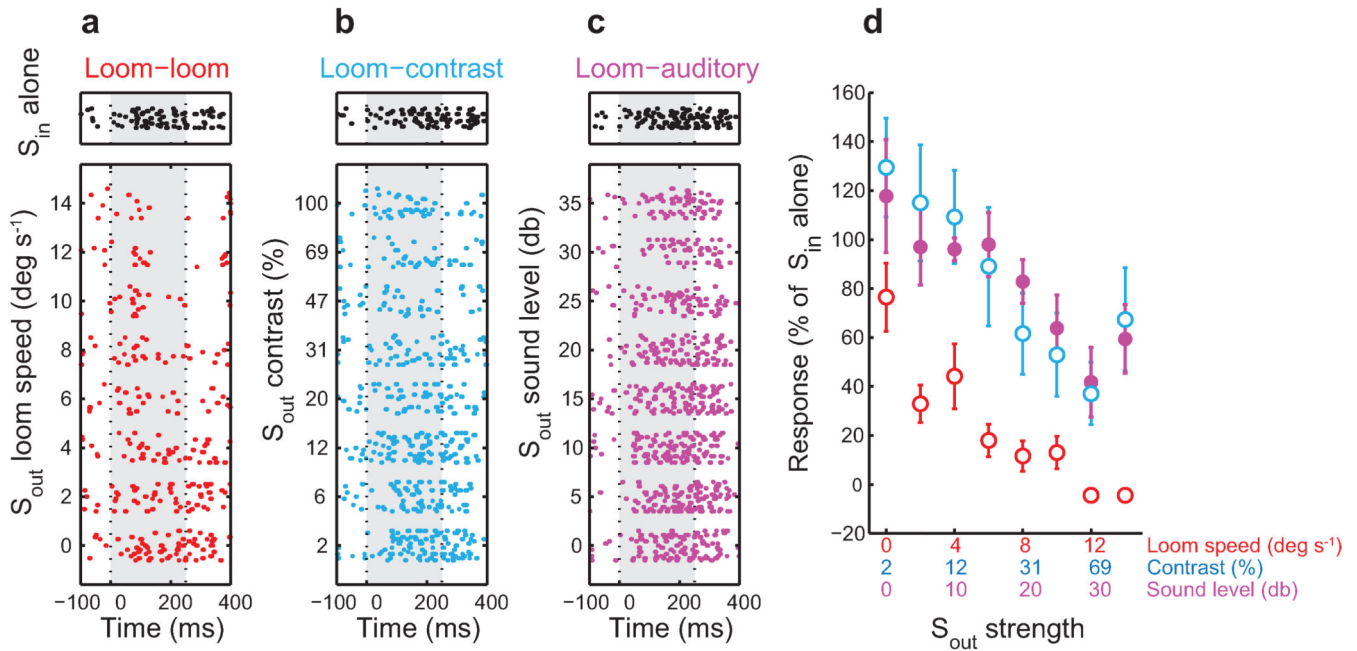


**Figure 1. Feature and modality independence of stimulus competition for a single nonswitch-like Ipc unit**

The effect of the strength of a competing stimulus on responses to a dark looming dot ( $S_{in}$ ), 80% contrast, 4 °/s, centered in the receptive field at left 11°, +8°. An  $S_{out}$  competitor stimulus was located 30° to the side of the receptive field, at left 41°, +8°. The stimuli were presented simultaneously from 0–250 ms. **a)** Upper raster: responses to the  $S_{in}$  stimulus presented alone. Lower rasters: responses to the  $S_{in}$  stimulus paired with an 80% contrast, looming dot  $S_{out}$  stimulus with various speeds. **b)** Responses to the  $S_{in}$  stimulus paired with a looming dot  $S_{out}$  stimulus (speed = 4 °/s) with various contrasts. **c)** Responses to the  $S_{in}$  stimulus paired with a broadband noise burst  $S_{out}$  stimulus at various sound levels relative to the unit's threshold. **d)** Responses to the  $S_{in}$  and  $S_{out}$  stimuli presented together relative to the response to the  $S_{in}$  stimulus alone plotted as a function of  $S_{out}$  strength. Red:  $S_{out}$  = visual loom speed. Blue:  $S_{out}$  = visual loom contrast. Magenta:  $S_{out}$  = auditory noise burst. Responses are normalized by the response to the  $S_{in}$  alone for each profile. All  $S_{out}$  stimuli systematically suppressed the response to the  $S_{in}$  stimulus alone ( $p < 0.05$ , correlation analysis). Error bars indicate s.e.m.

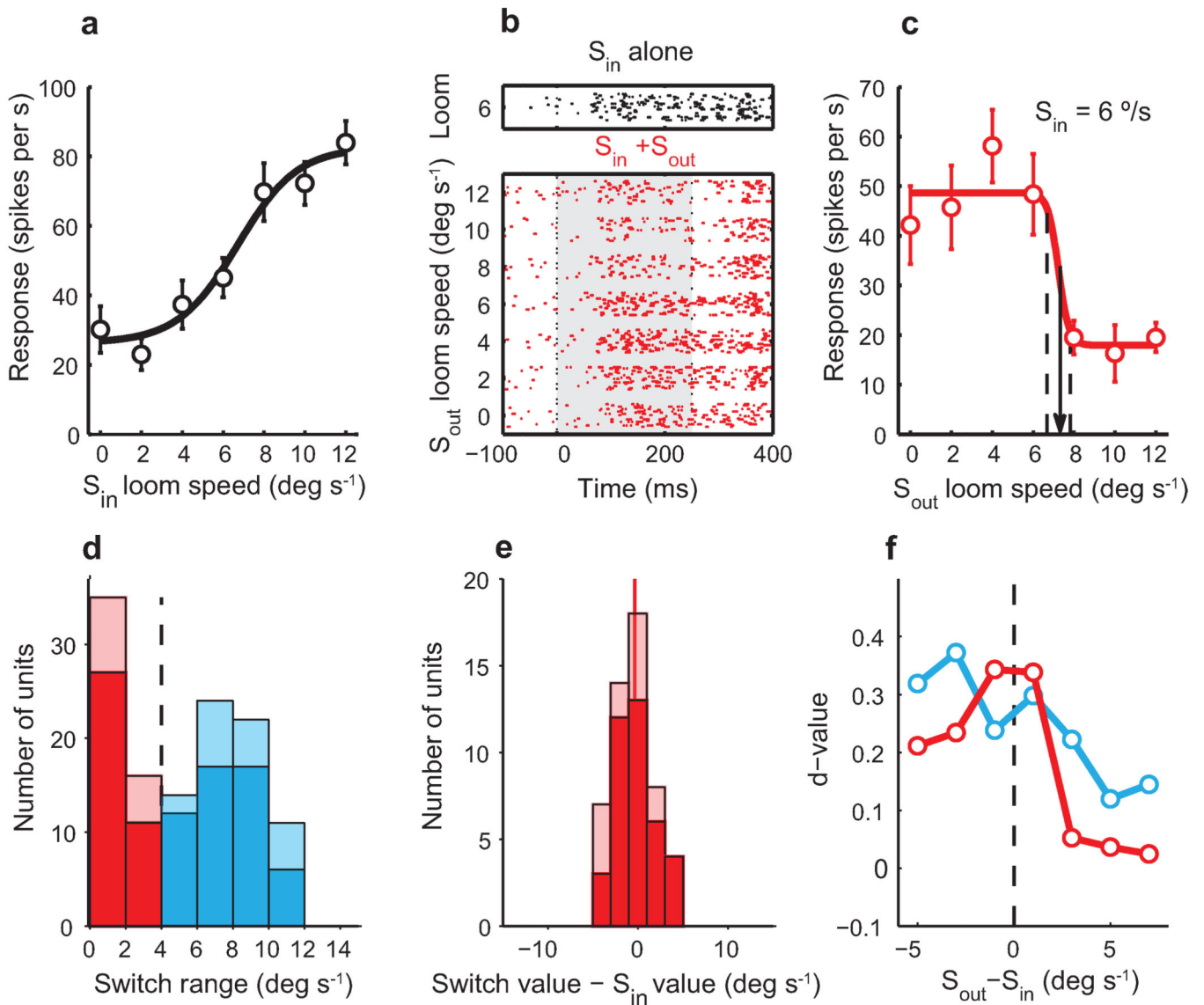


**Figure 2. Effect of a competing looming stimulus on unit responses to a looming stimulus**

**a)** Speed-response function for a single Ipc unit measured with a single looming stimulus centered in the receptive field. Line: sigmoidal fit to the data (Methods). **b)** Raster representation of the unit's responses to a looming  $S_{in}$  stimulus (6°/s) presented simultaneously with a looming  $S_{out}$  competitor of different loom speeds. **c)** The competitor strength-response profile: Mean response values for the responses shown in **b**. Line: sigmoidal fit to the data (Methods); dashed lines: transition range; arrow: switch value. This unit had a switch-like competitor strength-response profile. **d)** Distribution of transition ranges for 121 units tested with two looming stimuli; switch-like units (red) and non-switch-like units (blue). The light bars represent data from non-tranquilized owls. **e)** Distribution of differences between the switch value and the  $S_{in}$  loom speed for all switch-like units. Red line: mean difference =  $-0.32 \pm 0.39$  ( $p=0.3$ , Wilcoxon signed rank test,  $n=51$ ). The light bars represent data from non-tranquilized owls. **f)** Population average  $d'$  values comparing

responses to a 2 °/s increment in  $S_{out}$  value, plotted as a function of the average difference between the strengths of  $S_{out}$  and  $S_{in}$ . Red circles: data from switch-like units; blue circles: data from non-switch-like units. Error bars in **a** and **c** indicate s.e.m.

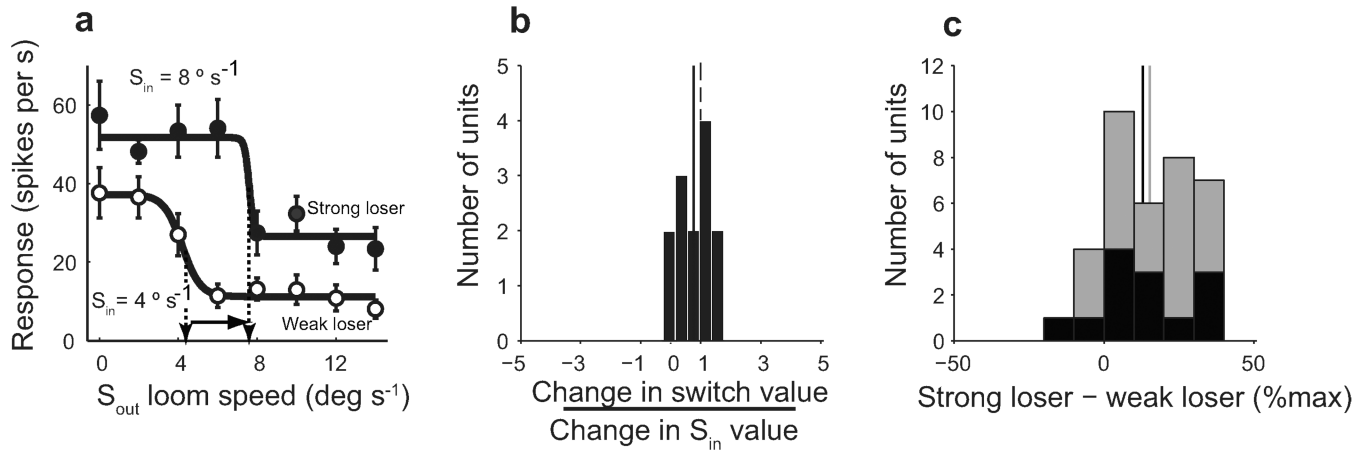


**Figure 3. Effect of the strength of the  $S_{in}$  stimulus on switch value**

**a)** Competitor strength-response profiles for a switch-like unit measured with two different  $S_{in}$  loom speeds: 4  $^\circ/s$  (open symbols) and 8  $^\circ/s$  (filled symbols). Solid lines: sigmoidal fits to the data; vertical arrows: switch values; horizontal arrow: change in switch value. Error bars indicate s.e.m. **b)** Ratio of the change in switch value relative to the change in  $S_{in}$  loom speed for switch-like units. All data measured with looming  $S_{in}$  and  $S_{out}$  stimuli. Dashed vertical line: designates one; Solid vertical line: mean ratio for switch units = 0.77; Wilcoxon signed rank test re. 1,  $n=13$ ,  $P=0.24$ . **c)** The difference between responses to a stronger, “loser”  $S_{in}$  stimulus versus a weaker, “loser”  $S_{in}$  stimulus. Black bars: switch-like units; gray bars: nonswitch-like units. For each unit, the difference is calculated as the average of the responses at  $S_{out}=12 \text{ } ^\circ/s$  and  $14 \text{ } ^\circ/s$ . The difference is expressed as a percentage of the maximum response to the stronger  $S_{in}$  stimulus presented alone. For switch-like units, an average increase in  $S_{in}$  strength of  $4.3 \pm 1.2 \text{ } ^\circ/s$  produced an average response increase of  $13 \pm 4.7\%$  (Wilcoxon signed rank test re. zero,  $n=13$ ,  $P=0.021$ ); for nonswitch-like units, an average increase in  $S_{in}$  strength of  $4.5 \pm 0.93 \text{ } ^\circ/s$  produced an average response increase of  $15.3 \pm 3.5\%$  (Wilcoxon signed rank test re. zero,  $n=23$ ,  $P<0.0001$ ). Black and gray vertical lines represents mean for switch-like and nonswitch-like neurons respectively.

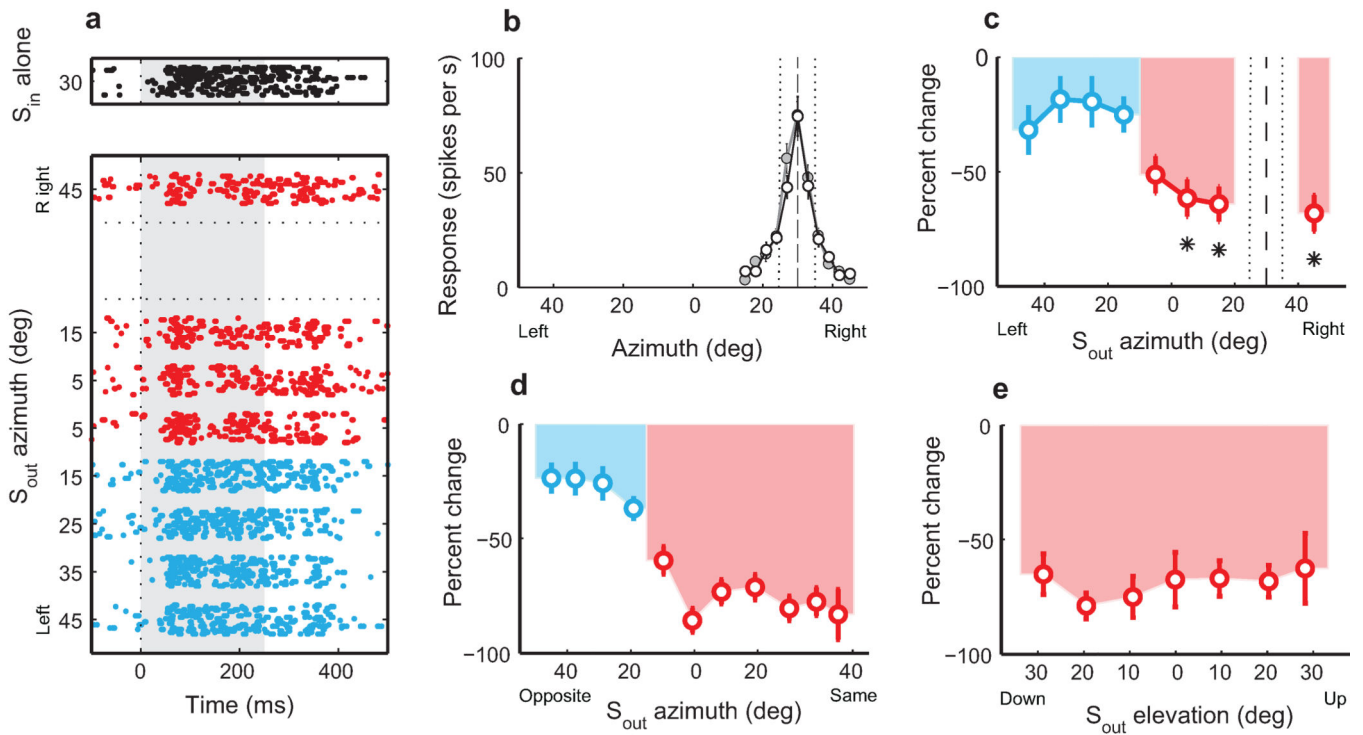


**Figure 4. Global stimulus competition in the Ipc**

**a)** Rasters of unit responses to a dark looming ( $4^\circ/s$ ) dot stimulus ( $S_{in}$ ), centered in the receptive field, with and without a competing,  $S_{out}$  looming stimulus ( $8^\circ/s$ ) presented from different azimuths. **b)** receptive fields of the unit to the  $S_{in}$  (black) and  $S_{out}$  (gray) stimuli presented alone. Dashed line: center of receptive field. Dotted lines: half-max. **c)** Response of the unit to the  $S_{in}$  and  $S_{out}$  stimuli presented together as a percent of the response to the  $S_{in}$  presented alone. Red circles: mean  $\pm$  s.e.m. for  $S_{out}$  locations  $<15^\circ$  into the hemifield opposite to the receptive field. Blue circles: mean  $\pm$  s.e.m. for  $S_{out}$  locations  $>15^\circ$  into the opposite hemifield. Dashed and dotted lines: receptive field. **d,e)** Population average suppression of responses to  $S_{in}$  as a function of the location of the  $S_{out}$  stimulus.  $S_{in} = 4$  or  $6^\circ/s$ ;  $S_{out} = 8$  or  $10^\circ/s$ ;  $n=31$ ; mean  $\pm$  s.e.m.  $S_{out}$  locations more  $>15^\circ$  from the receptive field center were binned to the nearest  $10^\circ$  increment. **d)**  $S_{out}$  locations in azimuth. Red and blue circles, as in **c**. **e)**  $S_{out}$  locations in elevation.

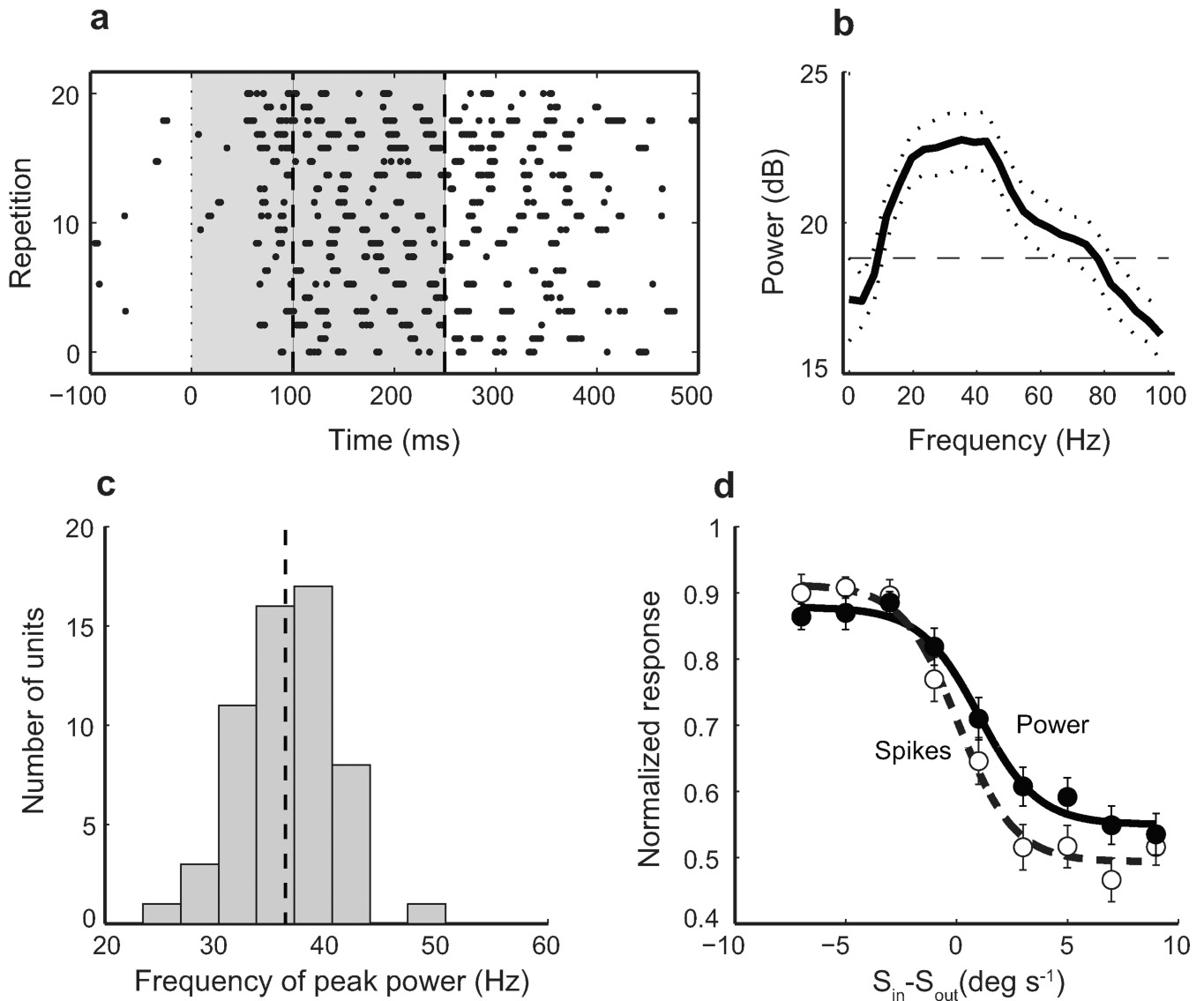


**Figure 5. Periodicity of bursting responses of Ipc units**

**a)** Raster of responses of an Ipc unit to an  $8^\circ/\text{s}$  looming stimulus centered in the receptive field. Dashed lines: response window analyzed for periodicity. **b)** Multi-taper spectral analysis of the spike pattern shown in **a** reveals a peak periodicity of 35 Hz. Solid line: mean power spectrum. Dotted lines: jackknife error bars. Dashed line: power spectrum of a hypothetical Poisson spiking neuron with equal firing rate. Deviation from the dashed line represents periodic nature of the phenomenon. **c)** Distribution of the peaks in the response power spectra for 57 Ipc units. Dashed line: mean  $\pm$  s.e.m:  $36.3 \text{ Hz} \pm 0.7$ . **d)** Covariation of average power of spike periodicity, measured in the 20–60 Hz band, and average spike rate for a population of 39 switch-like units, each responding to a looming  $S_{\text{in}}$  stimulus presented simultaneously with a looming  $S_{\text{out}}$  stimulus of different speeds. The abscissa shows the difference in strength between  $S_{\text{out}}$  and  $S_{\text{in}}$ . Error bars indicate s.e.m.